



Thermosensitive/magnetic molecularly imprinted polymers prepared by Pickering emulsion polymerization for selective separation of bifenthrin

Li Yang^a, Yao Chen^b, Jiangdong Dai^a, Naichao Si^c, Yongsheng Yan^{a,*}

^aSchool of Chemistry and Chemical Engineering, Jiangsu University, Zhenjiang 212013, China, Tel. +86 15050851390; email: yangli035@126.com (L. Yang), Tel. +86 15996848210; email: daijiangdong035@126.com (J. Dai), Tel. +86 13952922917; email: jdxz2011@126.com (Y. Yan)

^bSchool of the Environment and Safety Engineering, Jiangsu University, Zhenjiang 212013, China, Tel. +86 18361810962; email: chenyaoyao1390@163.com

^cSchool of Material Science and Engineering, Jiangsu University, Zhenjiang 212013, China, Tel. +86 13775365246; email: sinaochao035@163.com

Received 10 November 2014; Accepted 4 September 2015

ABSTRACT

Thermosensitive/magnetic molecularly imprinted polymers (TM-MIPs) were prepared by Pickering emulsion polymerization. With this method, SiO₂ nanoparticles were used as the Pickering emulsion stabilizer, N-isopropylacrylamide functioned as the thermosensitive monomer participating in co-polymerization, and bifenthrin (BF) acted as the template molecule. The results of the characterizations demonstrated that the TM-MIPs were porous and magnetic inorganic/polymer composite microparticles with magnetic sensitivity ($M_s = 0.7921 \text{ emu g}^{-1}$), thermal stability (below 473 K), and magnetic stability (over the pH range of 2.0–8.0). TM-MIPs were used as sorbents to remove bifenthrin (BF), and then were swiftly split in magnetic field. The Freundlich isotherm model preferably matched with the experimental data. The adsorption kinetic of the TM-MIPs was primely fitted by the pseudo-second-order, indicating that the chemical reaction could be the rate-limiting step in the process of BF absorption. The selective recognition experiments exhibited that the TM-MIPs have obvious effect on selective adsorption of BF with diethyl phthalate and fenvalerate. In aqueous solutions, the adsorption of BF onto the TM-MIPs had response to temperature, and could be used for adsorbing and separating bifenthrin.

Keywords: Thermosensitive molecularly imprinted polymers; Bifenthrin; Selective recognition; Pickering emulsion polymerization

1. Introduction

Pyrethroids were successfully developed as a kind of chemical synthesis broad-spectrum insecticides by mimicking the structures of natural pyrethrins, with stable properties, low effective concentration, strong

contact action, fast pest control, selective insecticidal activity, and so forth, which interfere with the mechanism of nerve conduction to leave pests to die [1]. In the past few decades, pyrethroids were widely used for controlling agricultural pests, healthy insects, and now they gradually take the place of organic phosphorus, organic nitrogen, and organic chlorine traditional insecticides in agriculture [2,3]. For

*Corresponding author.

example, bifenthrin was used to kill pests on vegetables, fruit trees, and tea trees. In recent years, pyrethroid pesticides have accounted for nearly 20% of the international pesticide market. Mass production and widespread use of pyrethroids, flowing into the environment through production wastewater, pesticide residue, and other methods resulted in environmental pollution and ecosystem destruction, which has aroused wide attention at home and abroad. Moreover, the research on migration, toxicology, biological hazards, and treatment methods of pyrethroids residue in the environment have been reported [4–7]. Some studies suggest that pyrethroids have influence on the central nervous system of human when confronting the consciousness obstacles and seizures, and the disruption of the endocrine system [8]. Therefore, how to separate pyrethroid residues rapidly and sensitively has become a hotspot in this field. Alternatively, adsorption is a kind of simple and effective approach to eliminate residual pyrethroids in the environment.

The materials of selective recognition and separation of pyrethroid compounds have stepped into the spotlight of research. Molecularly imprinted polymers (MIPs) are a type of selective adsorbent for the quick removal of target pollutants, and can be used for adsorption–desorption repeatedly when removing contaminants [9]. The magnetic separation technique is a quick and easy separation technique, which can replace centrifugation and filtration, and has been used in the molecular imprinting field [10]. Since temperature is the most common kind of stimulation, thermosensitive polymer can be adapted to temperature changes [11], wherein, poly-N-isopropyl acrylamide (PNIPAm) is studied most, whose low critical solution temperature is about 32°C [12]. Reversible phase transition has attracted extensive attention of researchers at home and abroad because of its occurrence by the temperature change. Zhang et al. prepared water-soluble MIPs with temperature stimulation effect by superficially grafting PNIPAm brush onto MIPs microspheres [13]. The intelligent control of template molecules adsorbed on thermosensitive MIPs can be implemented by adjusting the ambient temperature. In the field of separation science, drug delivery, catalysis, and sensing, thermosensitive MIPs have great application prospects.

Pickering emulsion polymerization technique is a novel method of preparing MIPs. Pickering emulsions use solid particles instead of surfactants as an emulsion stabilizer [14]. Recently, Pickering emulsion polymerization has been proven to be a green synthetic technique in terms of reducing the large amount of surfactants to prepare organic–inorganic hybrid microspheres, which has become a hot topic [15,16].

For example, clay-armored latexes were prepared by Pickering emulsion polymerization using clay as emulsion stabilizer [17].

In this work, thermosensitive and magnetic molecularly imprinted polymers (TM-MIPs) were successfully prepared by Pickering emulsion polymerization, and used as an adsorbent for the selective adsorption separation of bifenthrin (BF). As shown in Fig. 1, for preparing TM-MIPs, the template molecule was BF, the functional monomer was methacrylic acid (MAA), the thermosensitive monomer was N-isopropyl acrylamide (NIPAm), the cross-linking agent was ethylene glycol dimethacrylate (EGDMA), and the initiator was azobis isobutyrate dimethyl (AIBME). The mixture of BF, MAA, NIPAm, EGDMA, AIBME, toluene, and dichloromethane acted as oil phase. The oleic acid modified Fe₃O₄ nanoscale particles serving as the magnetic carrier was dispersed in the oil phase, SiO₂ nanoparticles working as the Pickering stabilizer was dispersed in aqueous phase, an oil-in-water Pickering emulsion was formed by severe shaking. Some relevant characterizations of the TM-MIPs were studied to analyze its physicochemical properties. The adsorption isotherm, kinetics, selectivity, and temperature response of BF were researched using the TM-MIPs as sorbents.

2. Experimental

2.1. Chemicals

Bifenthrin (BF) and fenvalerate (FL) were purchased from Jiangsu Huangma agrochemicals Co., Ltd. Ethanol, methanol, acetic acid, dichloromethane, HPLC-grade methanol, and methacrylic acid (MAA), FeCl₂·4H₂O, FeCl₃·6H₂O, NaOH, trimethylstearyl ammonium bromide, oleic acid, toluene, methylene chloride, and tetraethoxysilane (TEOS) were obtained from Sinopharm Chemical Reagent Co., Ltd (Shanghai, China). Ammonium hydroxide, N-isopropyl acrylamide (NIPAm), diethyl phthalate (DEP), dimethyl 2,2'-azobis(2-methylpropionate) (AIBME), and Ethyl glycol dimethacrylate (EGDMA) were received from Aladdin Reagent Co., Ltd (Shanghai, China). Deionized water (DI, 18.2 ML cm⁻¹) is obtained through a Milli-Q water purification system.

2.2. Instrument

Infrared spectra (4,000–400 cm⁻¹) were recorded on a Nicolet NEXUS-470 FTIR apparatus (USA). The morphology of TM-MIPs was observed by a scanning electron microscope (SEM, JEOL, JSM-7001F) and a transmission electron microscope (TEM, JEOL,

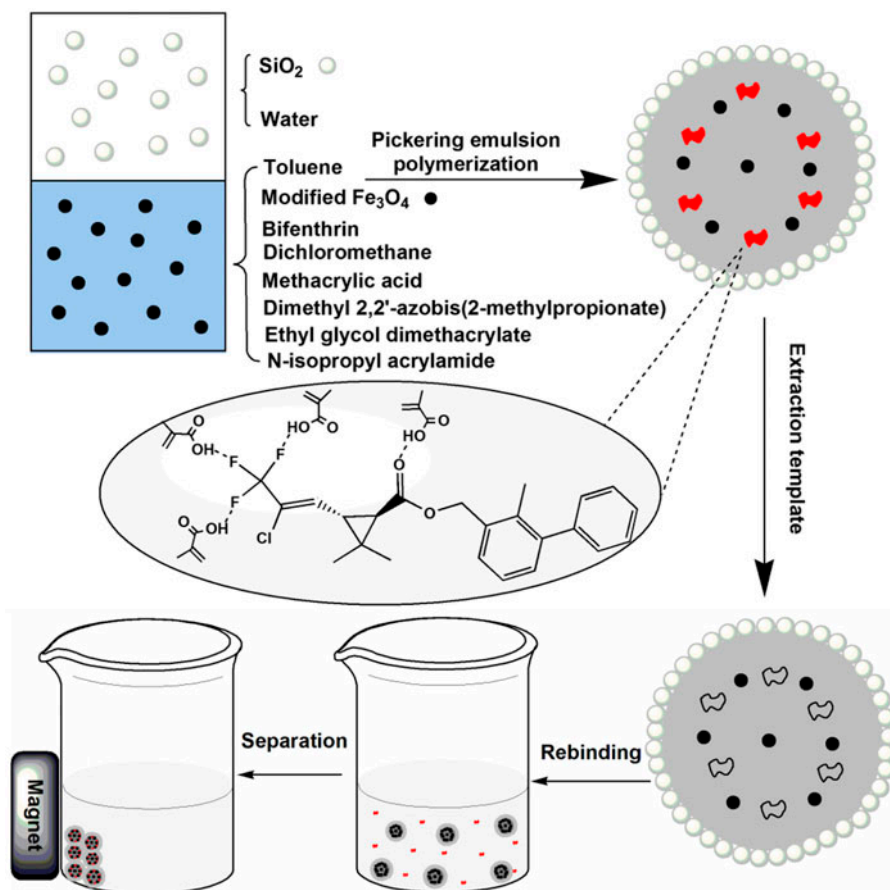


Fig. 1. The synthesis of TM-MIPs by Pickering emulsion polymerization.

JEM-2100). The identification of crystalline phase was performed using a Rigaku D/max- γ B X-ray diffractometer (XRD). Magnetic measurement was carried out using a vibrating sample magnetometer (VSM, 7300, Lakeshore). Thermogravimetric analysis (TGA) was carried out using a DSC/DTA-TG (STA 449C Jupiter, Netzsch, Germany) at N₂ atmosphere. A TBS-990 atomic absorption spectrophotometer (Beijing Purkinge General Instrument Co., Ltd, China) was used for ion measurements. Chromatographic analysis was carried out on an Agilent 1200 BF system (Agilent, Germany). UV–vis adsorption spectra were obtained from a UV–vis spectrophotometer (UV-2450, Shimadzu, Japan).

2.3. Preparation of SiO₂ nanoparticles

The preparation of SiO₂ nanoparticles was carried out referring to a method from Stöber et al. [18]. Briefly, 3.0 mL TEOS was added into 100 mL of ethanol and water (95:5, V/V) solution, followed by adding

0.01 g trimethylstearylammonium bromide, and the mixture was remained ultrasonic every one minute. 1.0 mL ammonium hydroxide diluted by 6.0 mL deionized water was slowly added dropwise to the above solution. After incubating at 25°C in a water bath for 6.0 h, the synthetic SiO₂ nanoparticles were gathered using high-speed centrifugation, washed with water and ethanol three times, and dried in 30°C vacuum.

2.4. Synthesis and surface oleic acid modification of Fe₃O₄ nanoparticles

Fe₃O₄ nanoparticles were synthesized according to the literature reported method from Massart [19]. In a typical run, 1.35 g FeCl₃·6H₂O and 0.6 g FeCl₂·4H₂O were dissolved in 50 mL deionized water, then the mixture was heated to 30°C, and mechanical stirred for 15 min in N₂ atmosphere. Subsequently, 50 mL of 0.5 mol L⁻¹ NaOH solution was added rapidly to the above solution with vigorous mechanical stirring for 20 min. The synthetic Fe₃O₄ nanoparticles were

separated by applied magnetic field, and washed with ethanol three times. The obtained Fe₃O₄ nanoparticles were dispersed in 40 mL mixture of oleic acid and ethanol (1:3, V/V), heated to 50°C, and mechanically stirred for 6.0 h. After magnetic separation, the hydrophobic Fe₃O₄ nanoparticles (HFNs) were washed with ethanol three times and dried in vacuum at 40°C.

2.5. Preparation of TM-MIPs

Firstly, 0.11 mg BF and 0.1 mL MAA were added to a mixed solution of 1.0 mL of toluene and 1.0 mL of dichloromethane for the pre-polymerization reaction. After 6.0 h, 1.0 mL EGDMA, 0.565 g NIPAm, 0.05 mL AIBME, and 0.05 g HFNs were added into the above solution and magnetically stirred for 10 min, and the mixture was used as the oil phase of Pickering emulsion. 0.35 g SiO₂ nanoparticles acting as Pickering emulsion stabilizers were dispersed in 20 mL deionized water. The stable oil-in-water (O/W) Pickering emulsion was prepared by vigorous shaking. After purging with N₂ for 10–20 min, the Pickering emulsion was heated to 65°C for 12 h. The synthetic TM-MIPs were collected by magnetic separation and washed by water and ethanol three times, subsequently dried in vacuum at 50°C. Finally, the template molecule (BF) with a mixture of methanol and acetic acid (95:5, V/V) were washed away. The obtained TM-MIPs were dried in vacuum at 50°C. The method of preparing corresponding thermosensitive magnetic non-imprinted polymer (TM-NIPs) was similar to TM-MIPs, but without adding template molecule BF in the preparation process. Corresponding non-thermosensitive magnetic imprinted polymers (NTM-MIPs) were not added into sensitive monomer NIPAm during the preparation process.

2.6. Static adsorption experiments

The influence of initial BF concentration (20–200 mg L⁻¹) and equilibration time (30–720 min) on the adsorption of BF was investigated. In the study of adsorption isotherm, 5.0 mg TM-MIPs or TM-NIPs were added into 10 mL ethanol and distilled water solutions (5:5, V/V) of BF at various concentrations. The temperature of the solutions was thermostatically controlled at 25°C. After 12 h, the TM-MIPs or TM-NIPs were isolated by an external magnetic field. In the study of adsorption kinetics, 10 mL solution with the initial BF concentration of 200 mg L⁻¹ was reacted with 5.0 mg of adsorbents in batch experiments, and the residual amount of BF in the water phase was measured using UV–vis spectrophotometer at 254 nm.

The amount of BF adsorbed (mg g⁻¹) at time t was calculated by a mass balance relationship:

$$Q_t = \frac{(C_0 - C_t)V}{W} \quad (1)$$

where C_0 is defined as the initial concentration of BF in the solution (mg L⁻¹), C_t represents the remaining concentration in the solution at time t (mg L⁻¹), V is the solution volume (L), and W stands for the adsorbent mass (g). When C_t is replaced by C_e is used instead of in Eq. (1), and Q_e is calculated.

2.7. Selective recognition experiments

The selective recognition of the TM-MIPs sorbents was evaluated using BF and another two structurally related compounds, DEP and FL, respectively. Firstly, single-solute adsorption was studied. 5.0 mg TM-MIPs or TM-NIPs sorbent was added into three colorimeter tubes, both containing 10 mL of 100 mg L⁻¹ BF, FL, or DEP. After adsorption at 25°C for 12 h, BF, FL, and DEP were detected by UV–vis spectrophotometer at 254, 277.5, and 275 nm, respectively. Afterwards, dual-solute solution was studied. The experiments were conducted by standing at 25°C for 12 h. A binary mixed solution containing BF, DEP, or FL was prepared with the same concentration of 100 mg L⁻¹. The experiment was carried out by adding 5.0 mg TM-MIPs or TM-NIPs into a colorimeter tube containing 10 mL of the binary mixed solution. The supernatant was separated from the colorimeter tubes, and analyzed by HPLC with UV detector at 254 nm. The samples were separated by a C₁₈ column in which the mobile phase was a mixture of 88% methanol and 12% deionized water, and the flow rate was 1.5 mL min⁻¹.

2.8. Temperature sensitive experiments

About 20 mg of adsorbents TM-MIPs and NTM-MIPs were added to 1.0 L of 0.1 mg L⁻¹ BF aqueous solution (deionized water as the solvent), keeping at different temperatures (25, 30, 35, 40, 45°C) in a water bath oscillator with a rate of 200 rpm for 24 h. The sorbent solution was collected by a permanent magnet, then added to 2.0 mL of ethanol elution and kept ultrasonic for 1.0 h. The BF concentration in the supernatant was tested by HPLC instrument equipped with an Agilent TC-C18(2) column (4.6 × 250 mm, 5.0 μm) and UV detector at 254 nm.

2.9. Regeneration

About 5.0 mg TM-MIPs used as adsorbents were added into 10 mL of 200 mg L⁻¹ BF solution,

maintained in 25°C water bath for 12 h. After adsorption, the TM-MIPs were separated using a permanent magnet. The supernatant was removed and tested by UV-vis spectrophotometer. The adsorbent TM-MIPs were washed with 2.0 mL eluent (methanol: acetic acid = 95:5, V/V) with ultrasonic eluted for three times and 10 min for each run. The as-prepared TM-MIPs were reused for four times.

2.10. Magnetite leakage experiments

To estimate the amount of magnetite that is likely to leach from TM-MIPs, 10 mg TM-MIPs was placed in test tubes containing 10 mL deionized water with different pH values (ranging from 2.0 to 8.0). The mixture was shaken by a rotary shaker for 12 h. Then, the TM-MIPs were isolated by an external magnetic field, and the amount of the iron ion leached into the media was measured by a graphite furnace atomic absorption spectrophotometer.

3. Results and discussion

3.1. Design and preparation of Pickering emulsion

Photos of Pickering emulsion before (a) and after (b) ultrasonification are shown in Fig. 2. The optical micrograph of the emulsion is shown in Fig. 2(c). Fig. 2(a), which suggests that the water phase dispersion with SiO₂ nanoparticles was located at the top of the vial, while the black oil phase dispersion was located at the bottom of the vial. After ultrasonification and emulsification, O/W Pickering emulsion could be obtained.

3.2. Characterization

The FT-IR spectra of SiO₂, Fe₃O₄, HFNs, TM-MIPs, and NTM-MIPs are shown in Fig. 3. SiO₂ infrared spectrum shows a broad peak at 3,387 cm⁻¹, which may be a stretching vibration peak of O-H on the surface of the silica. The peaks at 1,098 and 951 cm⁻¹ are characteristic absorption peaks of Si-O-Si and Si-OH, and the peaks at 801 and 467 cm⁻¹ are asymmetric stretching vibration absorption peaks of Si-O-Si [20]. Fe₃O₄ infrared spectroscopy shows two broad peak at 572 and 629 cm⁻¹, which are characteristic absorption peaks of Fe-O, proving the successful preparation of Fe₃O₄ nanoparticles [21,22]. Compared to Fe₃O₄, the absorption peaks of HFNs at 2,852 and 2,920 cm⁻¹ are attributed to the CH asymmetric stretching vibration of -CH₂ and -CH₃, indicating that oleic acid was successfully grafted on the surface of Fe₃O₄ nanoparticles.

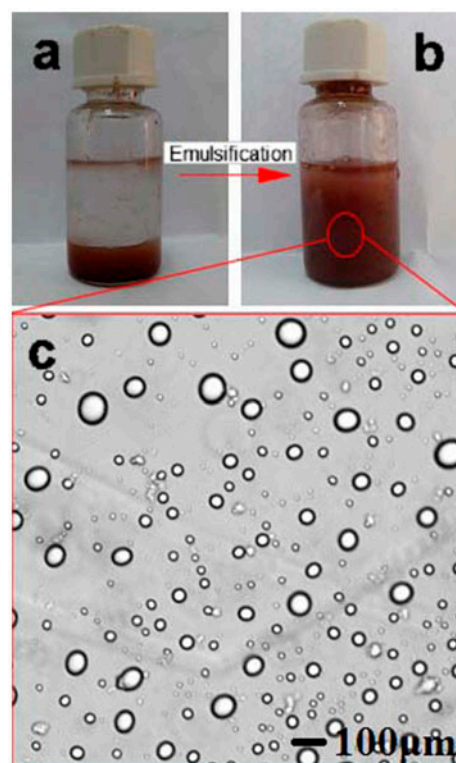


Fig. 2. Photos of Pickering emulsion before (a), after (b) ultrasonification and the optical micrograph of the emulsion (c).

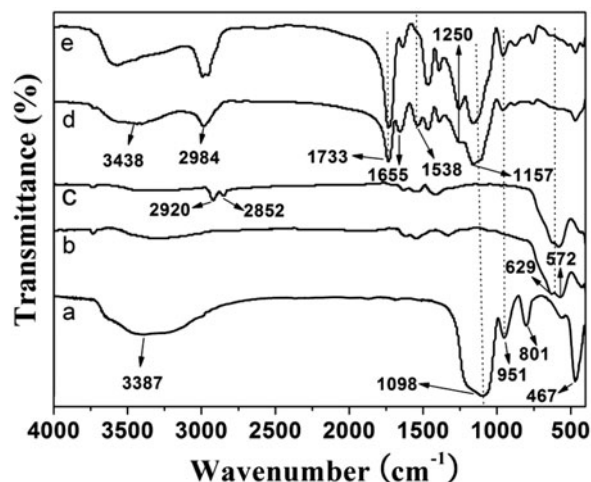


Fig. 3. FT-IR spectra of the SiO₂ (a), Fe₃O₄ (b), HFNs (c), TM-MIPs (d), and NTM-MIPs (e).

TM-MIPs infrared spectrum shows that the significant absorption peaks at 1,733, 1,655, 1,250, and 1,157 cm⁻¹ are stretching vibration of C=O, C=C, and symmetric and asymmetric stretching vibration peaks of C-O.

The absorption peak at $2,984\text{ cm}^{-1}$ is typical absorption peak of CH on CH_3 [23,24]. The broad absorption peak at $3,438\text{ cm}^{-1}$ is stretching vibration absorption peak of $-\text{NH}$ and OH . Compared with the NTM-MIPs, the characteristic absorption peak of TM-MIPs at $1,538\text{ cm}^{-1}$ is bending vibration absorption peak of NH on amide groups ($-\text{NHCO}$) [25], which illustrated that thermosensitive monomers NIPAm were successfully introduced to the polymer. These peaks proved the successful synthesis of TM-MIPs.

The EDX spectra (a) of TM-MIPs and XRD pattern (b) of Fe_3O_4 were measured and shown in Fig. 4. When 2θ is between 20° and 70° , there are six characteristic diffraction peaks of Fe_3O_4 , which illustrated that Fe_3O_4 was successfully prepared. In the EDX spectra of TM-MIPs (Fig. 4(a)), Si was from Pickering emulsion stabilizer SiO_2 , N was from thermosensitive monomer NIPAm, C was from the imprinted polymer, and Fe was from the magnetic carrier Fe_3O_4 . All these show that the TM-MIPs were successfully prepared.

The TGA curves of TM-MIPs and TM-NIPs are shown in Fig. 5. When the temperature was lower than 200°C , the loss quality of TM-MIPs and TM-NIPs was due to the absorbed water. When the temperature was between 200 and 800°C , the mass loss quality of TM-MIPs and TM-NIPs resulted from the decomposition of the polymer network at a high temperature. Finally, the Fe_3O_4 , SiO_2 , and residual carbonized polymers were left. The organic mass percentage of TM-MIPs and TM-NIPs was only 1.1%, which was mainly due to different degrees of polymerization. With the temperature increased to 800°C , the significant weight losses of TM-MIPs and TM-NIPs could be seen, respectively. At 800°C , the remaining mass for

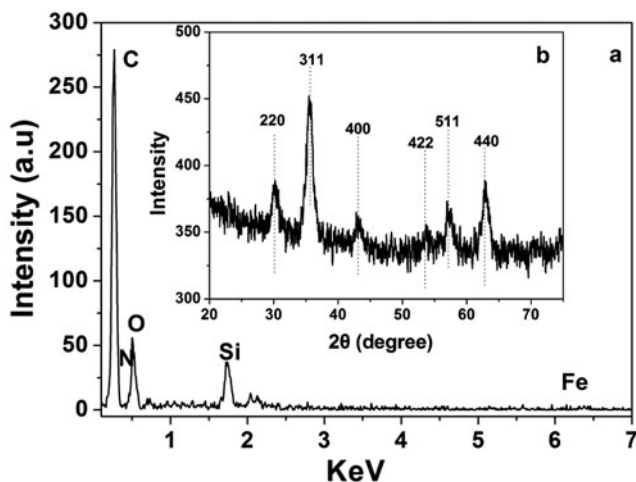


Fig. 4. EDX spectra of the TM-MIPs (a) and XRD pattern of the Fe_3O_4 nanoparticles (b).

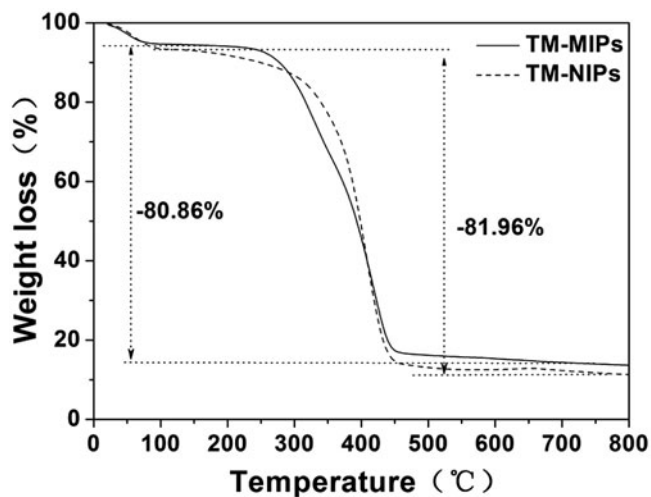


Fig. 5. TGA curves of the TM-MIPs and TM-NIPs.

TM-MIPs and TM-NIPs may be attributed to the thermal resistance of residual carbon by calcining polymers. The TGA curves of TM-MIPs and TM-NIPs had the same trend, indicating they possessed similar morphological structure and size distribution.

TM-MIPs magnetic properties are shown in Fig. 6. Hysteresis loop displayed the magnetic saturation and intensity of Fe_3O_4 in the TM-MIPs are 54.13 and 0.79 emu g^{-1} , respectively. Magnetic separation diagram shows that TM-MIPs could be successfully and magnetically separated, which reflected that the synthetic TM-MIPs were magnetic. Magnetic leakage

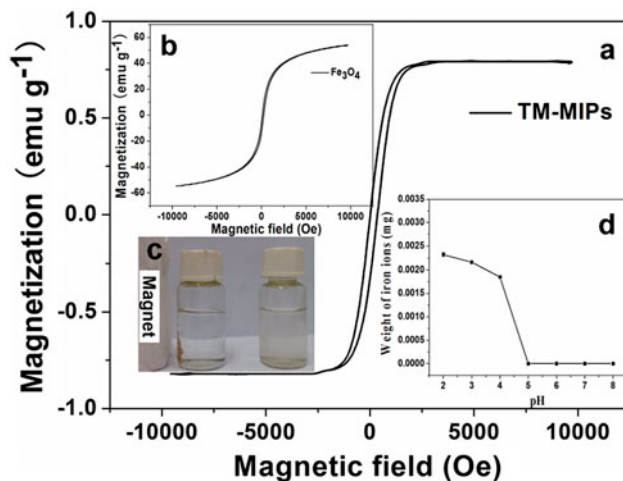


Fig. 6. Magnetization curves obtained by VSM at room temperature of TM-MIPs (a) and Fe_3O_4 (b), a photograph of the TM-MIPs dispersed in the water in the presence (left) and absence (right) of an external magnetic field (c), and magnetite leakage curve of the TM-MIPs (d).

figure shows that at $\text{pH} \geq 4$, almost no magnetic material leaked. Even when the pH 2, only 0.0023 mg of iron ion was detected in the supernatant, which illuminated that TM-MIPs have certain magnetic stability.

Morphology of Fe_3O_4 nanoparticles and SiO_2 nanoparticles were observed by TEM, which can be seen from Fig. 7(a) and (b), the size of SiO_2 nanoparticles was approximately 50 nm in diameter, and the size of Fe_3O_4 nanoparticles was about 15 nm in diameter. The morphology of TM-MIPs was observed by SEM, and the diameter of TM-MIPs particles ranged from 10 to 60 μm . The enlarged view of the surface of TM-MIPs shows many SiO_2 nanoparticles were on the surface, which illustrated SiO_2 nanoparticles were successfully attached to the surface of the polymer microspheres. From the section graph of TM-MIPs, it can be concluded that a plurality of holes were inside the polymer, and the diameter was at about 20–200 nm. The resulting description of TM-MIPs proves that it has a porous structure.

3.3. Adsorption isotherm

Theoretically, the binding properties of the TM-MIPs and TM-NIPs for BF were studied by the equilibrium adsorption experiments, and the equilibrium data fitting to the Langmuir and Freundlich isotherm models are shown in Fig. 8. The Langmuir isotherm presupposes that the adsorption behavior is based on

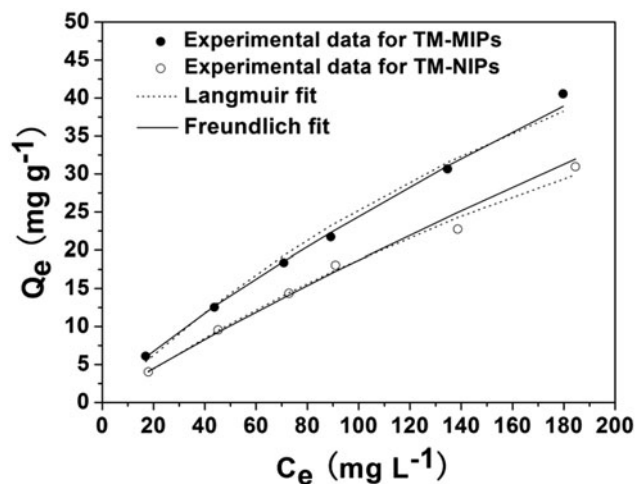


Fig. 8. Equilibrium data and modeling for the adsorption of BF onto the TM-MIPs and TM-NIPs.

monolayer adsorption and homogeneous solid surface, while the Freundlich isotherm is an empirical equation which assumes a heterogeneous surface energy and uneven solid surface [26]. The applicability of the isotherm models to the adsorption behaviors was studied by judging the correlation coefficient (R^2). The nonlinear form of the Langmuir and Freundlich isotherm models is expressed by the following equations, respectively [27,28]:

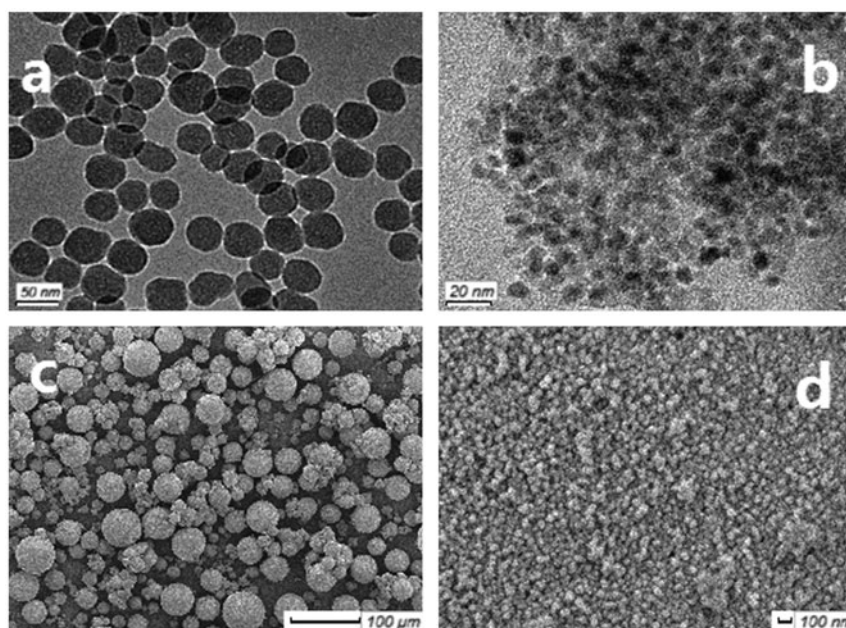


Fig. 7. TEM images of the SiO_2 nanoparticles (a) and Fe_3O_4 nanoparticles (b), a SEM image (c), the surface with magnification image (d) and a profile image (e) of the TM-MIPs.

Table 1

Langmuir and Freundlich adsorption isotherm constants for BF onto the TM-MIPs and TM-NIPs

Adsorption isotherm modes	Constants	TM-MIPs	TM-NIPs
Langmuir equation	R^2	0.8293	0.8917
	Q_m (mg g ⁻¹)	105.2632	99.0099
	K_L (L mg ⁻¹)	0.003173	0.002343
Freundlich equation	R^2	0.9986	0.9952
	K_F (mg g ⁻¹)	0.6296	0.3199
	$1/n$	0.7943	0.3199

$$Q_e = \frac{K_L Q_m C_e}{1 + K_L C_e} \quad (2)$$

$$Q_e = K_F C_e^{1/n} \quad (3)$$

where Q_e (mg g⁻¹) is the equilibrium adsorption capacity, C_e (mg L⁻¹) is the equilibrium concentration of the adsorbate at equilibrium, and Q_m (mg g⁻¹) is the maximum adsorption capacity of the sorbent. K_L (L mg⁻¹) is the Langmuir adsorption constant. K_F (mg g⁻¹) is the Freundlich adsorption equilibrium constants, and $1/n$ is a measure of exchanging intensity or surface heterogeneity, with a value of $1/n$ smaller than 1.0 describing favorable removal conditions [29]. All calculated values of the adsorption experiment are listed in Table 1.

As seen in Fig. 8, the adsorption capacity increased with the increasing concentration of BF. In addition, the adsorption capacity of TM-MIPs was higher than that of TM-NIPs under the same condition, which indicates the significant preferential adsorption of TM-MIPs for BF. It was probably due to good specificity of the TM-MIPs for the imprinted molecules [30]. The Freundlich isotherm model gave a better fit to the experimental data. Values of Freundlich constant $1/n$ (less than 1.0) are shown in Table 1, which indicated that the experimental conditions were favorable to BF adsorption. The calculated R^2 (Table 1) and the fitted curves (Fig. 8) fully illustrated that the binding of BF by the TM-MIPs and TM-NIPs was compatible with the Freundlich isotherm model. In a controlled experiment, sorbent obtained from MIPs that were further immersed in the HF solution to remove the SiO₂ layer revealed the maximum adsorption capacity of 106.1678 mg g⁻¹, which was similar with that of prepared MIPs in this work. This result suggested that SiO₂ layer on the surface of MIPs had no effect on the adsorption and mass transfer process.

3.4. Adsorption kinetics

The kinetics of adsorption is important because of the relation to process efficiency. In this study, the pseudo-first-order and pseudo-second-order were applied to investigate the controlling mechanism of the adsorption of BF onto TM-MIPs or TM-NIPs. The results are shown in Fig. 9 at initial concentration of 200 mg L⁻¹ and temperature of 25°C. The equilibrium time required for the adsorption of BF was about 640 min for TM-MIPs and TM-NIPs. The pseudo-first-order and pseudo-second-order kinetic models [31,32] can be expressed as Eqs. (4) and (5):

$$\ln(Q_e - Q_t) = \ln Q_e - k_1 t \quad (4)$$

$$\frac{t}{Q_t} = \frac{1}{k_2 Q_e^2} + \frac{t}{Q_e} \quad (5)$$

In the equations, Q_t (mg g⁻¹) and Q_e (mg g⁻¹) are the amount of BF adsorbed at time t and at equilibrium,

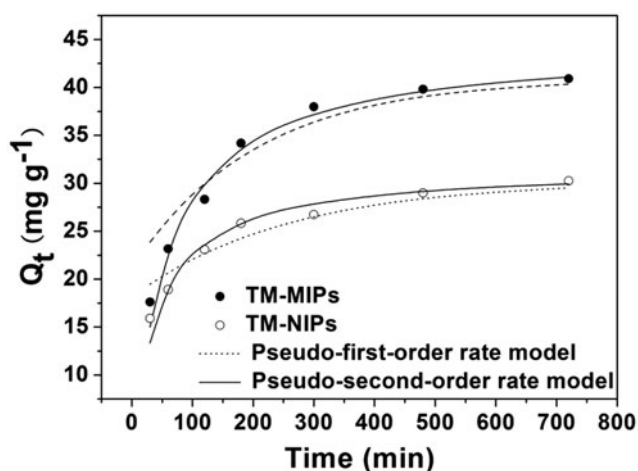


Fig. 9. Kinetic data and modeling for the adsorption of BF onto the TM-MIPs and TM-NIPs.

Table 2
Kinetics constants for the pseudo-first-order and pseudo-second-order rate equations

Adsorption kinetics modes	Constants	TM-MIPs	TM-NIPs
Pseudo-first-order equation	R^2	0.9045	0.9273
	$Q_{e,c}$ (mg g^{-1})	19.76	13.22
	k_1 (L min^{-1})	0.0049	0.0041
Pseudo-second-order equation	R^2	0.9992	0.9989
	$Q_{e,c}$ (mg g^{-1})	44.05	31.65
	k_2 (g (mg min)^{-1})	0.000428	0.000768
	h (mg (g min)^{-1})	0.8308	0.7692
	$t_{1/2}$	53.03	41.14

respectively. k_1 (min^{-1}) and k_2 ($\text{g mg}^{-1} \text{min}^{-1}$) are rate constants of the pseudo-first-order and pseudo-second-order, which can be calculated from the plots of $\ln(Q_e - Q_t)$ vs. t and t/Q_t vs. t . All rate constants of adsorption and linear regression correlation coefficients are presented in Table 2. As illustrated in Table 2, the pseudo-second-order kinetic model (R^2 values above 0.99) yielded a better fit than the pseudo-first-order for the adsorption of BF onto both TM-MIPs and TM-NIPs. It was assumed that the chemical process could be the rate-limiting step in the adsorption process for BF [33]. These results showed that the formation of specific recognition sites on the surface of TM-MIPs is beneficial for BF to be bounded. Based on the pseudo-second-order kinetic model, h (the initial adsorption rate, $\text{mg g}^{-1} \text{min}^{-1}$)

and $t_{1/2}$ (the half equilibrium time, min) are calculated as follows [34]:

$$h = k_2 Q_e^2 \quad (6)$$

$$t_{1/2} = \frac{1}{k_2 Q_e} \quad (7)$$

The initial adsorption rate and the half equilibrium time are usually applied in measurement of the adsorption rate. The results are summarized in Table 2. It further suggested that the TM-MIPs had more excellent kinetic property. The initial adsorption rate of BF onto TM-MIPs was higher than that of TM-NIPs.

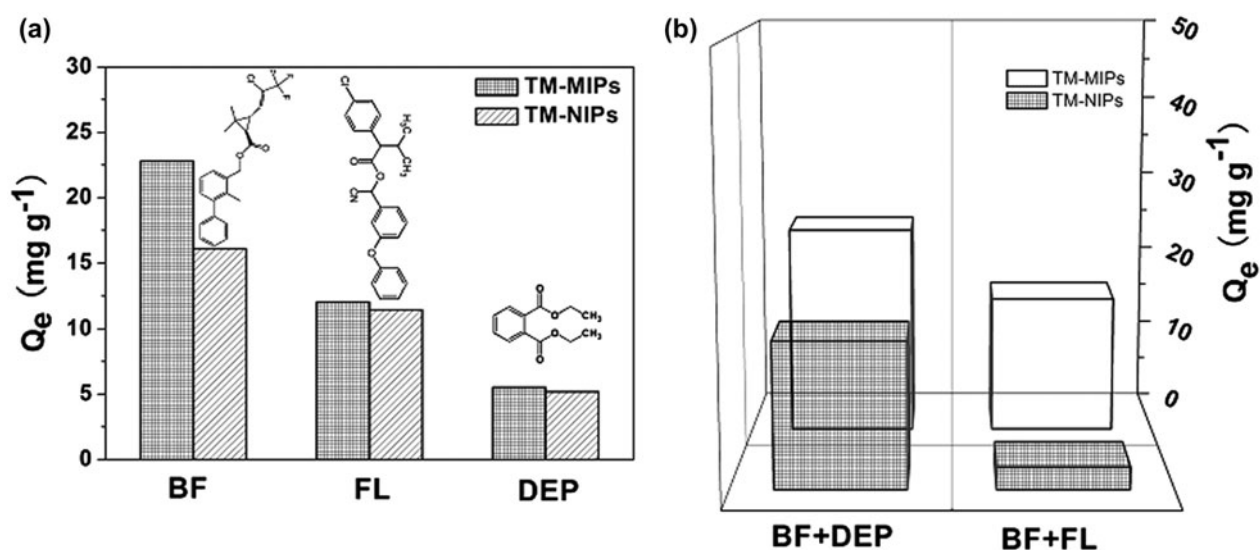


Fig. 10. (a) Adsorption capacity of the TM-MIPs and TM-NIPs for BF, FL, and DEP. Inset the structures of the test compounds, (b) adsorption selectivity of the TM-MIPs, and TM-NIPs for BF in dual-solute solution.

3.5. Selectivity analysis

The aim of the experiments was to demonstrate the feasibility that the TM-MIPs could selectively recognize BF from mixtures. To measure this specificity of the TM-MIPs on BF, the adsorption to BF was compared with DEP and FL, respectively. The molecular structures of these adsorbates (BF, DEP, and FL) were similar but also different to some extent, which are shown in Fig. 10(a). There was no obvious difference in the removal rates between the TM-MIPs and TM-NIPs for DEP or FL, and the TM-MIPs had much higher adsorption capacity for BF, indicating that the TM-MIPs had the selective recognition for the template molecule (BF). Hydrogen bond could be formed between the testing compounds and functional monomers. Through comparison of the adsorbates' chemical structural formulas, the different recognition effect may be due to the distinct sizes, structures, and functional groups of the templates [35]. To further investigate the adsorption selectivity of the TM-MIPs for the templates, DEP or FL was added into BF aqueous solution respectively to form dual solute solutions. Fig. 10(b) indicates that the TM-MIPs still exhibited a high removal rate for BF in the presence of competitive compounds, and the specific adsorption of the TM-MIPs for BF was also obvious, suggesting that the specific adsorption of the TM-MIPs for BF was not significantly affected by the competitive antibiotics. The TM-MIPs had the selective recognition for BF even in the presence of competitive antibiotics. The recognition sites of the imprinting cavities were not complementary to the competitive molecules (DEP and FL). What is more, in the aspects of space structure and the number of hydrogen bonds formed between adsorbates and imprinting cavities, BF had the most hydrogen bonds and was the best match with the imprinting cavities, leaving others less chance to be captured onto the TM-MIPs, which verified that the memory of specific functional groups also played an important role in the conformation memory [36].

3.6. Temperature-sensitive research

TM-MIPs were added into thermosensitive monomers NIPAm during the polymerization, having a temperature response characteristic (Fig. 11). When the temperature was below responsive temperature, TM-MIPs were hydrophilic and beneficial for aqueous approach into the polymer. After the temperature was above responsive temperature, TM-MIPs were hydrophobic and hindered aqueous solution into the interior of polymer. Temperature-sensitive experiments were carried out using 20 mg sorbent of

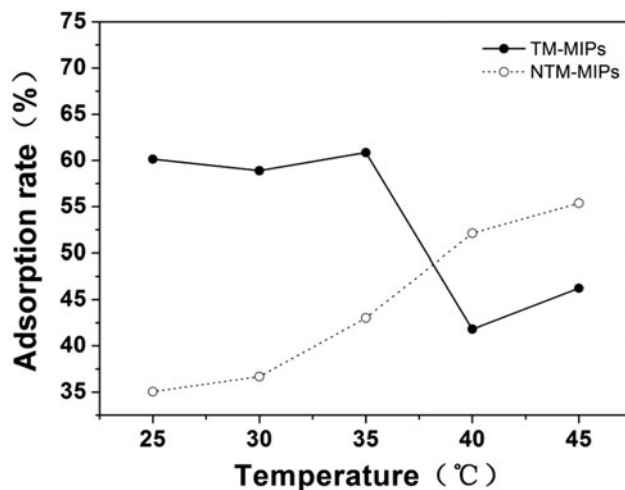


Fig. 11. The temperature effect on adsorption of BF onto TM-MIPs and NTM-MIPs in aqueous solution.

TM-MIPs and NTM-MIPs adsorpt by treating 1 L of 0.1 mg L^{-1} BF aqueous solution under different temperature. The results are shown in Fig. 11, and from 25 to 45°C, the adsorption rate of NTM-MIPs for BF in aqueous solution increased along with the increase in temperature. It illustrated that the adsorption process was an endothermic reaction. However, when the temperature ranges were 25–35 and 40–45°C, the adsorption rate of TM-MIPs for BF changed a little with temperature changes, adsorption rate at low temperature was larger than that at high temperature. From 35 to 40°C, the adsorption rate vigorously reduced by 19.05 percent with the increase in temperature. This was mainly caused by the dramatic change of the TM-MIPs surface wettability near the lowest critical temperature of the thermosensitive monomer NIPAm. This showed that the adsorption of TM-MIPs for BF did have temperature-sensitive effect. Therefore, the prepared adsorbent in this work could be controlled by adjusting the temperature.

3.7. Regeneration

Regeneration is important for the performance of an adsorbent. To make an evaluation of adsorbent regeneration, the experiment of adsorption–desorption was studied over four cycles using TM-MIPs prepared in this work. The adsorption capacity of the adsorbent TM-MIPs is shown in Fig. 12. After four times of adsorption, the adsorption capacity of the adsorbent TM-MIPs reduced by only 8.623%, probably in that the binding sites were damaged or collapsed during the repeated use of the process. Experimental results showed that TM-MIPs could be reused for adsorption.

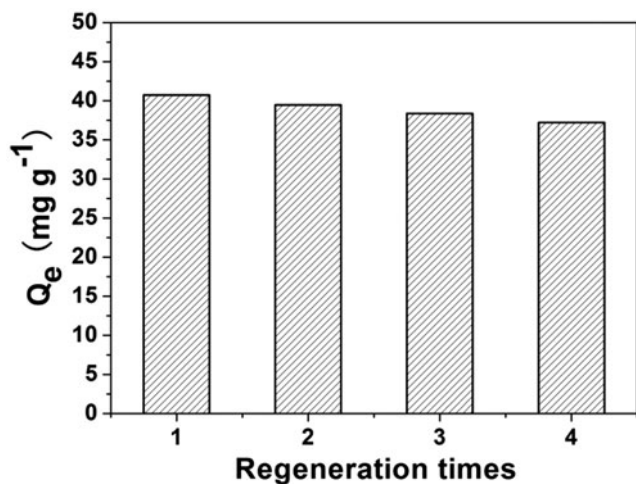


Fig. 12. Regeneration of the TM-MIPs for four cycles.

4. Conclusions

Thermosensitive/magnetic molecularly imprinted polymers (TM-MIPs) were successfully synthesized by Pickering emulsion polymerization, and were further applied in the selective adsorption of BF from aqueous solutions. SiO₂ nanoparticles provided Pickering emulsion with good stabilizer, and HFNs supplied magnetism to the TM-MIPs. Static adsorption experiments investigated the adsorption equilibrium and dynamic behavior of the TM-MIPs. The Freundlich isotherm model yielded a better fit than the Langmuir model for BF adsorbed onto the TM-MIPs and TM-NIPs. The kinetics of adsorption followed the pseudo-second-order model. In selective recognition experiments, the TM-MIPs proved to be endowed with better specific recognition and selectivity to BF even in the mixed solution. In addition, the adsorption of bifenthrin onto the MIPs had response to the temperature in water.

Acknowledgments

This work was financially supported by the National Natural Science Foundation of China (numbers 21107037 and 21176107), China Postdoctoral Science Foundation (No. 2012M521015) Natural Science Foundation of Jiangsu Province (numbers BK2011461, BK2011514, BK20131259), Postdoctoral Science Foundation funded Project of Jiangsu Province (No. 1202002B), Innovation Programs Foundation of Jiangsu Province (CXZZ12_0669), and Programs of Senior Talent Foundation of Jiangsu University (No. 12JDG090).

References

- [1] M.L. Feo, A. Ginebreda, E. Eljarrat, Presence of pyrethroid pesticides in water and sediments of Ebro River Delta, *J. Hydrol.* 393 (2010) 156–162.
- [2] D.M. Soderlund, D.C. Knipple, The molecular biology of knockdown resistance to pyrethroid insecticides, *Insect Biochem. Mol. Biol.* 33 (2003) 563–577.
- [3] M. Narendra, G. Kavitha, A. Helah Kiranmai, Chronic exposure to pyrethroid-based allethrin and prallethrin mosquito repellents alters plasma biochemical profile, *Chemosphere* 73 (2008) 360–364.
- [4] E.L. Amweg, D.P. Weston, N.M. Ureda, Use and toxicity of pyrethroid pesticides in the Central Valley, California, USA, *Environ. Toxicol. Chem.* 24 (2005) 966–972.
- [5] D.P. Weston, R.W. Holmes, J. You, Aquatic toxicity due to residential use of pyrethroid insecticides, *Environ. Sci. Technol.* 39 (2005) 9778–9784.
- [6] U. Friberg-Jensen, L. Wendt-Rasch, P. Woin, Effects of the pyrethroid insecticide, cypermethrin, on a freshwater community studied under field conditions. I. Direct and indirect effects on abundance measures of organisms at different trophic levels, *Aquat. Toxicol.* 63 (2003) 357–371.
- [7] T. Liu, C. Sun, N. Ta, Effect of copper on the degradation of pesticides cypermethrin and cyhalothrin, *J. Environ. Sci.* 19 (2007) 1235–1238.
- [8] G. Du, O. Shen, H. Sun, Assessing hormone receptor activities of pyrethroid insecticides and their metabolites in reporter gene assays, *Toxicol. Sci.* 116 (2010) 58–66.
- [9] A. Venkatesh, N. Chopra, R.J. Krupadam, Removal of acutely hazardous pharmaceuticals from water using multi-template imprinted polymer adsorbent, *Environ. Sci. Pollut. R* 3 (2014) 1–9.
- [10] S. Shi, J. Guo, Q. You, Selective and simultaneous extraction and determination of hydroxybenzoic acids in aqueous solution by magnetic molecularly imprinted polymers, *Chem. Eng. J.* 243 (2014) 485–493.
- [11] X.Y. Liu, Y. Guan, X.B. Ding, Design of temperature sensitive imprinted polymer hydrogels based on multiple-point hydrogen bonding, *Macromol. Biosci.* 4 (2004) 680–684.
- [12] H.G. Schild, M. Muthukumar, D.A. Tirrell, Cononsolvency in mixed aqueous solutions of poly(N-isopropylacrylamide), *Macromolecules* 24 (1991) 948–952.
- [13] G. Pan, Y. Zhang, X. Guo, An efficient approach to obtaining water-compatible and stimuli-responsive molecularly imprinted polymers by the facile surface-grafting of functional polymer brushes via RAFT polymerization, *Biosens. Bioelectron.* 26 (2010) 976–982.
- [14] S.U. Pickering, Emulsions, *J. Chem. Soc., Trans.* 91 (1907) 2001–2021.
- [15] X. Li, C. Zhu, Y. Wei, Fabrication of macroporous foam and microspheres of polystyrene by Pickering emulsion polymerization, *Colloid Polym. Sci.* 292 (2014) 115–122.
- [16] H. Zhou, T. Shi, X. Zhou, Poly (vinyl alcohol)/SiO₂ composite microsphere based on Pickering emulsion and its application in controlled drug release, *J. Biomater. Sci.-Polym. E* 25 (2014) 1–16.

- [17] S. Cauvin, P.J. Colver, S.A.F. Bon, Pickering stabilized miniemulsion polymerization: Preparation of clay armored latexes, *Macromolecules* 38 (2005) 7887–7889.
- [18] W. Stöber, A. Fink, E. Bohn, Controlled growth of monodisperse silica spheres in the micron size range, *J. Colloid Interface Sci.* 26 (1968) 62–69.
- [19] R. Massart, Preparation of aqueous magnetic liquids in alkaline and acidic media, *IEEE Trans. Magn.* 17 (1981) 1247–1248.
- [20] X. Qiu, Z. Fang, B. Liang, Degradation of decabromodiphenyl ether by nano zero-valent iron immobilized in mesoporous silica microspheres, *J. Hazard. Mater.* 193 (2011) 70–81.
- [21] R.D. Waldron, Infrared spectra of ferrites, *Phys. Rev.* 99 (1955) 1727–1735.
- [22] M. Ma, Y. Zhang, W. Yu, H.Y. Shen, H.Q. Zhang, N. Gu, Preparation and characterization of magnetite nanoparticles coated by amino silane, *Colloids Surf., A* 212 (2003) 219–226.
- [23] K. Yoshimatsu, K. Reimhult, A. Krozer, Uniform molecularly imprinted microspheres and nanoparticles prepared by precipitation polymerization: The control of particle size suitable for different analytical applications, *Anal. Chim. Acta* 584 (2007) 112–121.
- [24] S. Gam-Derouich, M. Ngoc Nguyen, A. Madani, Aryl diazonium salt surface chemistry and ATRP for the preparation of molecularly imprinted polymer grafts on gold substrates, *Surf. Interface Anal.* 42 (2010) 1050–1056.
- [25] S. Kovačič, K. Jeřabek, P. Krajnc, Responsive poly (acrylic acid) and poly(N-isopropylacrylamide) monoliths by high internal phase emulsion (HIPE) templating, *Macromol. Chem. Phys.* 212 (2011) 2151–2158.
- [26] X. Wang, J.M. Pan, W. Guan, J.D. Dai, X.H. Zou, Y.S. Yan, C.X. Li, W. Hu, Selective removal of 3-chlorophenol from aqueous solution using surface molecularly imprinted microspheres, *J. Chem. Eng. Data* 56 (2011) 2793–2801.
- [27] S.J. Allen, G. McKay, J.F. Porter, Adsorption isotherm models for basic dye adsorption by peat in single and binary component systems, *J. Colloid Interface Sci.* 280 (2004) 322–333.
- [28] M. Mazzotti, Equilibrium theory based design of simulated moving bed processes for a generalized Langmuir isotherm, *J. Chromatogr. A* 1126 (2006) 311–322.
- [29] H.Y. Zhang, A.M. Li, J. Sun, P.H. Li, Adsorption of amphoteric aromatic compounds by hyper-cross-linked resins with amino groups and sulfonic groups, *Chem. Eng. J.* 217 (2013) 354–362.
- [30] J.M. Pan, H. Yao, L.C. Xu, H.X. Ou, P.W. Huo, X.X. Li, Y.S. Yan, Selective recognition of 2,4,6-trichlorophenol by molecularly imprinted polymers based on magnetic halloysite nanotubes composites, *J. Phys. Chem. C* 115 (2011) 5440–5449.
- [31] Y.S. Ho, G. McKay, The sorption of lead(II) ions on peat, *Water Res.* 33 (1999) 578–584.
- [32] Y.S. Ho, G. McKay, Pseudo-second order model for sorption processes, *ProcessBiochem.* 34 (1999) 451–465.
- [33] G. Baydemir, M. Andaç, N. Bereli, R. Say, A. Denizli, Selective removal of bilirubin from human plasma with bilirubin-imprinted particles, *Ind. Eng. Chem. Res.* 46 (2007) 2843–2852.
- [34] Z.J. Wu, H. Joo, K. Lee, Kinetics and thermodynamics of the organic dye adsorption on the mesoporous hybrid xerogel, *Chem. Eng. J.* 112 (2005) 227–236.
- [35] Y. Chang, T. Ko, T. Hsu, M. Syu, Synthesis of an imprinted hybrid organic–inorganic polymeric sol–gel matrix toward the specific binding and isotherm kinetics investigation of creatinine, *Anal. Chem.* 81 (2009) 2098–2105.
- [36] Q. Yu, S.B. Deng, G. Yu, Selective removal of perfluorooctane sulfonate from aqueous solution using chitosan-based molecularly imprinted polymer adsorbents, *Water Res.* 42 (2008) 3089–3097.